# A Millennial-Scale Oscillation in Latitudinal Temperature Gradients along the Western North Atlantic during the Mid-Holocene

**Bryan N. Shuman[1], Ioana C. Stefanescu[1], Laurie D. Grigg[2], David R. Foster[3], and W. Wyatt Oswald[4]**

[1] Department of Geology and Geophysics, University of Wyoming, Laramie, WY.

[2] Department of Earth and Environmental Sciences, Norwich University, Northfield, VT.

[3] Harvard Forest, Harvard University, Petersham, MA.

[4] Marlboro Institute for Liberal Arts and Interdisciplinary Studies, Emerson College, Boston, MA.

Corresponding author: Bryan Shuman (bshuman@uwyo.edu)

**Key Points:**

- A major ecotone in eastern North America, which is linked to the latitudinal temperature gradient, shifted repeatedly during the Holocene.
- Pollen-inferred temperatures from different latitudes across the ecotone reveal gradient responses to deglaciation and orbital change.
- Changes at 4.8-3.8 ka also indicate millennial-scale variability with patterns analogous to the North Atlantic Oscillation.

## Abstract

Changes in vegetation in North America indicate Holocene shifts in the latitudinal temperature gradient along the western margin of the North Atlantic. Tree taxa such as oak (*Quercus*) and birch (*Betula*) experienced opposing directions of change across different latitudes consistent with changes in temperature gradient steepeness. Pollen-inferred temperatures from 34 sites quantify the gradient changes and reconstruct a long-term northward steepening in summer and southward steepening in winter. From 4.8-3.8 ka, an oscillation in tree distributions interrupted the long-term trends as a steep temperature gradient developed north of 43.5°N. The shift likely limited cold outbreaks to the south, producing anomalously high summer temperatures at 42-43.5°N, and enabling a northward expansion of oak forests. The forest and temperature gradient changes appear consistent with orbital and ice sheet forcing as well as millennial variability in the North Atlantic pressure field analogous to the North Atlantic Oscillation on interannual time scales.



## Plain Language Summary

In the Northern Hemisphere, average temperatures decline with latitude as climates cool toward the pole. Changes in this temperature pattern have significant consequences for weather systems and ecosystems. Past changes likely impacted the geographic extent of summer warmth and winter freezing that can determine where tree species can grow. In this study, fossil evidence of ancient tree distributions revealed how the poleward temperature gradient near the Atlantic coast of North America fluctuated over the past 11,700 years. Long-term forest and temperature changes developed in response to the deglaciation of Canada and Earth's slow orbital changes. However, a particularly striking change 4800-3800 years ago briefly expanded oak-hickory forests into mid-latitude highlands otherwise dominated by cold-tolerant northern tree species. The forest histories demonstrate the potential for ecosystems to change rapidly in the future, but also how fossil records can reveal poorly understood patterns and processes of millennial-scale climate variability. Temperature patterns detected here may be analogous to patterns of climate variability in the North Atlantic region at monthly-to-annual scales.

## 1 Introduction

In the northern mid-latitudes, temperatures decline steeply poleward. The areas of greatest change along the polar front are associated with westerly jet streams and eco-climatic transition zones (Bryson, 1966). Their location depends upon topography and surface conditions (Pielke & Vidale, 1995; Seager et al., 2002), but climate variability such as the North Atlantic Oscillation (NAO) can modify the summer and winter patterns (Folland et al., 2009; Hurrell et al., 2003). Orbital changes (Davis & Brewer, 2009; Routson et al., 2019), the intensity of oceanic overturning circulation (Fastovich et al., 2020; Levesque et al., 1997) and the demise of the Laurentide ice sheet have also produced long-term changes near the North Atlantic (COHMAP, 1988; Shuman et al., 2002). Additional changes likely developed at millennial scales based on data from the North Atlantic (Larsen et al., 2012; Orme et al., 2021), Europe (Fletcher et al., 2013; Vannière et al., 2011), and North America (Shuman et al., 2019). In eastern North America, oxygen isotopes indicate a rapid southward shift in the polar front in the mid-Holocene (Kirby et al., 2002) when coastal pollen records indicate abrupt changes from Virginia to Massachusetts (Willard et al., 2005; Foster et al., 2006). However, patterns and processes of abrupt and millennial-scale climate variation during the Holocene have been hard to diagnose (Crucifix et al., 2017), potentially because shifts in gradients and frontal movements can create opposing changes and areas of no change in close geographic proximity.

The sentivity of Holocene tree distributions to both growing season warmth and winter freezing temperatures can help reconstruct the past temperature gradients (Prentice et al., 1991; Woodward, 1987). In eastern North America near the North Atlantic, an ecotone between mixed and broadleaf forests expressed a close association with temperature at the time of European colonization (Cogbill et al., 2002; Thompson et al., 2013). It angled across the northeast U.S., approximating the orientation of today's 8°C mean annual isotherm with respect to latitude, topography, and proximity to the ocean (Cogbill et al., 2002). However, its position shifted throughout the Holocene (Oswald et al., 2018) and the earliest palynological studies inferred temperature changes from these ecotone dynamics (Deevey, 1939). Because direct comparisons reveal a tight coupling between fossil pollen and independent paleoclimate data (Shuman et al., 2019), the dense network of fossil pollen stratigraphies in the northeast U.S. (Fig. 1a) may help to document patterns and timescales of Holocene changes in the latitudinal temperature gradient (LTG) where it is sensitive to the NAO (Fig. 1b-e).

Oak (*Quercus* spp.) and hickory (*Carya* spp.) tree populations dominate the broadleaf forests south of the ecotone and may be particularly useful indicators of past changes in the LTG. The tree distributions define the ecotone where they trade-off in dominance with cool-tolerant taxa such as birch (*Betula* spp.) and hemlock (*Tsuga canadensis*) to the north (Cogbill et al., 2002). Additionally, oak and hickory differ in their seasonal temperature sensitivities. They have similar distributions in the northeast U.S. today, but strikingly different historic distributions in the central U.S. where continental summer and winter temperature gradients differ from each other; cold continental winters limit hickory's northern extent more than that of oak (Paciorek et al., 2016, 2021; Prentice et al., 1991). Changes in the geography of these trees therefore may provide insight into Holocene changes in the LTG in both summer and winter, including in association with a long-debated regional decline in hemlock abundance (Davis, 1981; Foster et al., 2006; Booth et al., 2012).

Here, we use a dense network of 34 pollen stratigraphies to infer summer and winter temperature changes at different latitudes across the northeast U.S. Mean annual temperatures

range from <2°C to >12°C across the study area today (Fig. 1a), but we reconstruct changes both in the absolute range and the shape of the gradient. We evaluate the reconstructions by comparing them with the regional histories of oak, hickory, birch, and hemlock. The major patterns of change highlight the ecological significance of millennial-scale climate variability near the North Atlantic.

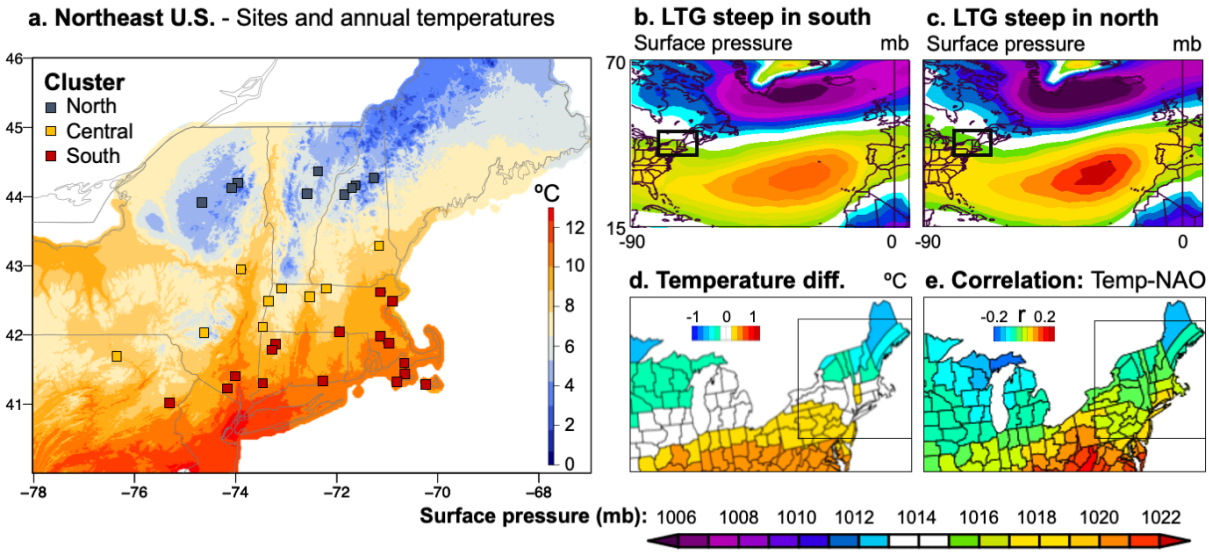


**Figure 1. The fossil pollen sites (square symbols in a) span the gradient of modern mean annual temperatures in the northeast U.S. Additional maps represent modern variability in the latitudinal temperature gradient (LTG) in the study region (inset boxes in b-e). Maps of composite mean surface atmospheric pressures show years when the LTG was steepest b) south of 42.75°N (1960, 1977, 1988, 1999, 2001) and c) north of 42.75°N (1954, 1959, 1968, 1991, 2007). Lower maps represent d) the associated composite mean temperature differences (LTG steep in north minus steep in south) and e) the correlation coefficeient, r, between the NAO and mean annual temperature (T) in each U.S. climate division (Vose et al., 2014). Modern mean annual temperatures across the region (a) are based on 1991-2020 PRISM normals (PRISM 2020); symbol colors indicate the geographical cluster containing each fossil site. See Supplementary Information for composite anomaly methodology.**

## 2 Methods

Detailed fossil pollen records from Connecticut, Massachusetts, New Hampshire, New York, Pennsylvania, and Vermont were obtained from the Neotoma Paleoecological Database (Williams et al., 2018). The records were selected from areas that span the full north-south temperature contrast between 40-45°N latitude. This range of latitudes was possible from 70-77°W longitude, but not in places to the east, such as Maine. To ensure a wide sampling of the regional patterns (particularly in the north), we included all radiocarbon dated records that span at least the past 8 ka (Table S1). We account for uncertainities tied to varying chronological

control and sample frequency, and reduce local ecological noise, through as much replication as possible within latitudinal zones and averaging the different time series.

Temporal resolution of the records ranges from >750 to <10 years per sample (95% range) with a median resolution of 124 years per sample. Chronologies were updated using *Intcal20* in *bchron* (Parnell et al., 2008; Reimer et al., 2020). Past comparisons of radiocarbon ages from bulk sediment and terrestrial macrofossils in the same cores in this region reveal few differences, reducing the need to remove older records from the synthesis (Marsicek et al., 2013). Although no records stand out as substantial outliers, we identify one highly-resolved record from each of three latitude zones to verify that the major LTG patterns do not depend upon confounding elevation-temperature relationships, sampling resolution, or age control. The three highly-resolved records have similar elevations (300-400 m), sampling frequency ($1\sigma$ range of 45-158 yrs/sample) and age control measured by accelerator mass spectrometry (AMS); they derive from Sutherland Pond, New York (Maenza-Gmelch, 1997a), Little Pond, Royalston, Massachusetts (Oswald et al., 2018), and Knob Hill Pond, Vermont (Oswald et al., 2018).

We reconstructed mean summer (June-August) and winter (December-February) temperatures using the modern analog technique following Marsicek et al. (2013). We compared each fossil sample to all possible modern analogs from North America east of 95°W using the squared-chord distance metric (Overpeck et al., 1985). The modern pollen samples and their associated temperatures derive from Whitmore et al. (2005). For each fossil pollen sample, the temperatures of the best seven modern analogs were averaged to produce the reconstructed temperature using the R package, *rioja* (Juggins, 2019).

Hierarchical cluster analysis of the summer temperature reconstructions (*hclust* based on Euclidean distances in R)(R Core Development Team, 2022) was used to group the individual records into three ensembles. The clusters were determined from the consistency in their summer temperature reconstructions, which break out by latitude with northern (>43.5°N), central (42-43.5°N), and southern (<42°N) groups of sites, except that eastern coastal sites cluster with the southern group (Fig. 1a). The grouping is consistent with the angled orientation of the LTG today because of its interaction with both topography and proximity to the coast (Fig. 1a). The LTG reconstructions were based on the averages of all individual records within each group, but we confirm the patterns using the three records with similar elevations of 300-400 m. Reconstructions were first interpolated to 50-yr intervals to enable averaging.

The position of the steepest portion of the LTG was calculated as the change in temperature between latitude bands by measuring the mean temperature differences among clusters. We calculated both the mean central-northern (C-N) and southern-central (S-C) temperature difference through time. The two segments were then compared to detect where the LTG was steepest by subtracting the C-N and S-C differences from each other. Positive values in the C-N minus S-C difference indicate a steeper gradient north of 42.75°N, the mid-point of the region, and negative values indicate a steeper gradient to the south.

## 3 Results

### 3.1 Reconstructed temperature trends

All of the temperature reconstructions indicate significant early Holocene warming in both summer (Fig. 2) and winter (Fig. 3). At ca. 11.7 ka, the range of summer temperatures

increased from 15-16°C to 17.5-18.5°C with all latitudes warming by similar amounts. Summer warming peaked in the central and northern sites by 8 ka at 18-19°C, but southern sites continued to warm, reaching 21°C at 5.5 ka (Fig. 2). In winter, all three regions continued to warm until 5.5 ka (Fig. 3). After 10 ka, however, the southern sites warmed faster in winter than the central and northern sites; by 5.5 ka, southern sites reached near freezing (0°C) even though northern areas only warmed to -5°C (Fig. 3).

After the mid-Holocene, summer temperatures declined in both the northern and southern regions, but not at central sites, which were affected by a significant millennial-scale variation at 4.8-3.8 ka (Fig. 2). Initially, at 6.2 ka, northern sites cooled by 0.5°C in both summer (Fig. 2) and winter (Fig. 3). Then, by 4.8 ka, central sites warmed 0.5°C in summer (Fig. 2) and 1°C in winter (Fig. 3). Some northern sites then warmed again by a similar amount from 3.4-1.8 ka (thin blue lines, Fig. 2c, 3c), but rapid summer cooling of 0.5°C at 1.8 ka further prevented most northern sites from returning to their previous high temperatures. The three best-resolved records from similar elevations (thin lines, Fig. 2d, 3d) show patterns consistent with the inherently smoothed regional means (bold lines, Fig. 2d, 3d).

### 3.2 Reconstructed gradient changes

Qualitative interpretation of the fossil pollen record supports the infered gradient changes. Oak, which flourishes today where summer temperatures exceed 17°C (Williams et al., 2006), reached its maximum in the north by 9-8 ka when birch, a dominant northern pollen type, declined to a minimum (Fig. 2, green lines). Northern oak abundance then fell to near zero, even as it continued to increase in the south where birch was uncommon. The opposite direction of oak and birch change in the north and south from 9-5.5 ka, observed over many sites, indicate a widening difference in growing conditions. The temperature reconstructions based on the full pollen assemblages suggest that the overall temperature difference between north and south increased by 1-1.5°C (Fig. 2e).

The history of the central region differs from both north and south. Oak abundance also reached an early Holocene peak there as the ecotone shifted far north, but oak then declined before forming a second millennial-scale peak during a northward shift in the ecotone from 4.8-3.8 ka (Fig. 2b, green lines). The distinctive peak developed when oak abundance remained low in the north. The vegetation gradient thus steepened to the north because birch, rather than oak, reached a mid-Holocene maximum (Fig. 2c).

Unlike the oak and birch changes, the regional hemlock decline affected the central and northern areas similarly (Fig. 3b,c). Average birch abundance initially increased in both areas after 5.5 ka, but it then declined in the central region as oak increased by 4.8 ka (Fig. 2b). Beech (*Fagus grandifolia*), another cool-tolerant tree, experienced a similar brief peak from 5.5-4.8 ka at central sites (Fig. 4a). The mid-Holocene warmth that accompanied the subsequent oak maximum reduced the summer temperature gradient in the south (S-C) by 0.5°C but increased the northern gradient (C-N) by >1°C (Fig. 2e).

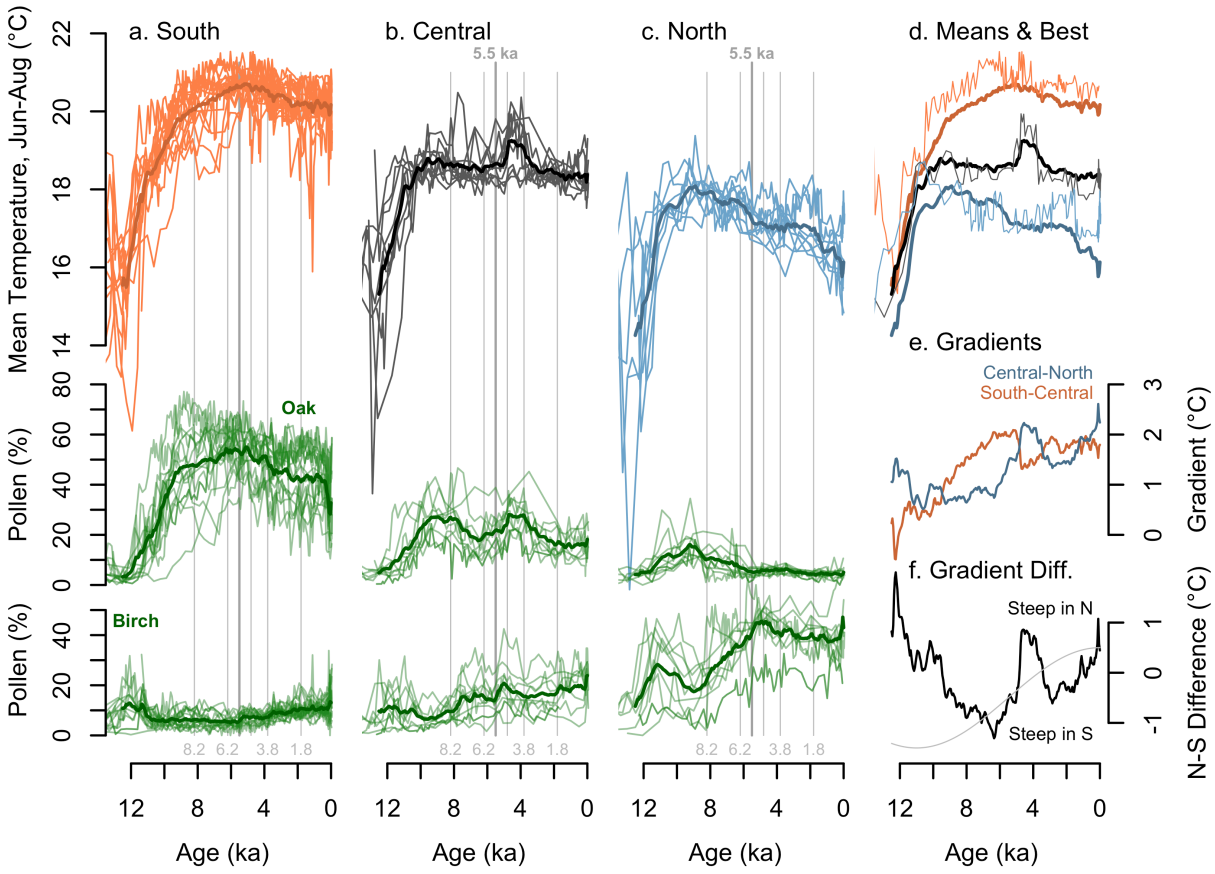


**Figure 2. Mean summer (June-August) temperatures as well as oak (*Quercus*) and birch (*Betula*) pollen percentages from a) southern, b) central, and c) northern sites. Mean reconstructions for each cluster (bold lines) as well as the best resolved records within the 300-400 m elevation zone (thin lines) are shown in (d) along with the mean differences between clusters (e) and the north minus south difference in gradient steepness ("Gradient Diff." as the black line in f). An inverted June insolation curve for 30°N (Berger, 1978) is normalized to the gradient difference scale for comparison (thin line, f). Vertical gray lines mark major time periods of change with the bold line at 5.5 ka indicating the median beginning of the regional hemlock decline (see Fig. 3). The vertical gray line at 4.8 ka is unlabeled.**

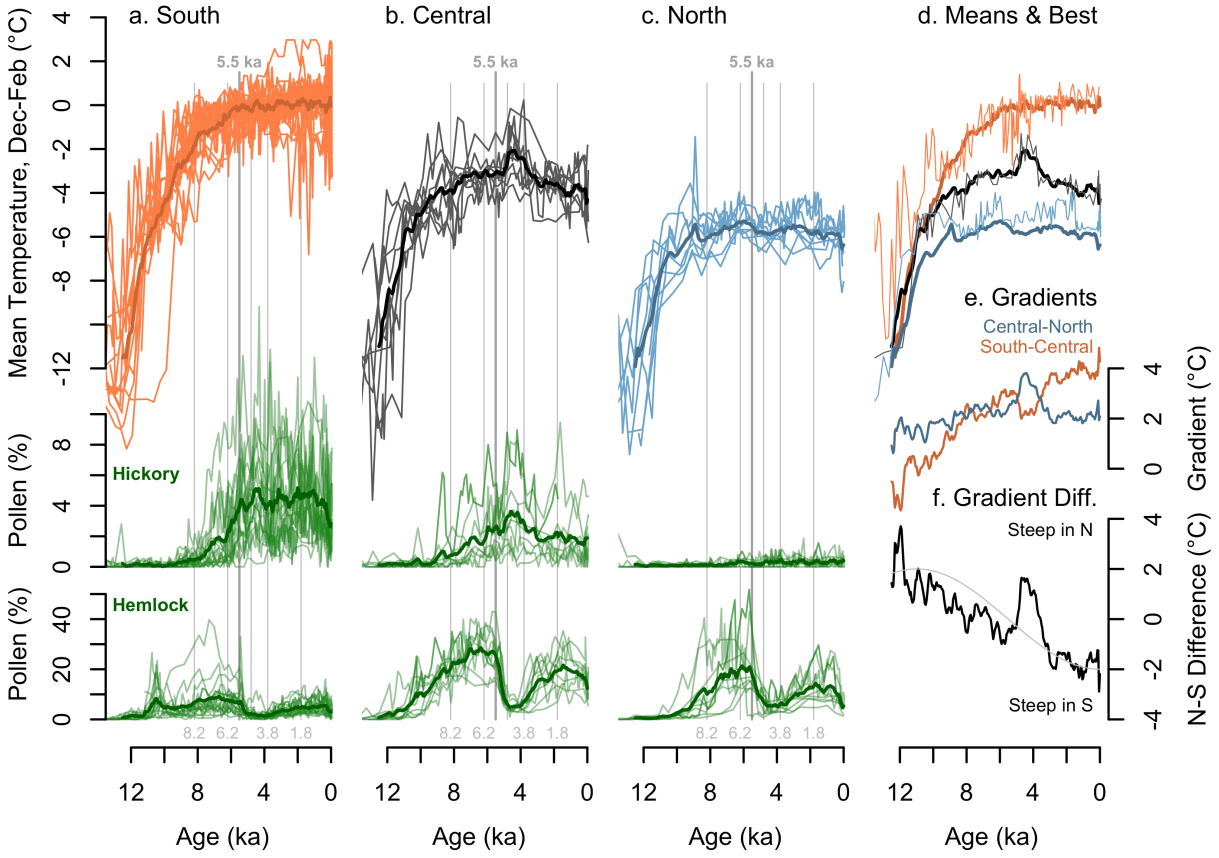


**Figure 3. As in Figure 2, but for mean winter (December-February) temperatures, hickory (*Carya*) and hemlock (*Tsuga*) pollen. A January insolation curve for 30°N (inverted, gray line) is normalized to the N-S gradient difference in f for comparison.**

The reconstructed gradients also changed in winter. The patterns appear qualitatively in the Holocene history of hickory (*Carya*), a genus of broadleaved deciduous trees usually restricted to areas today with mean winter temperatures greater than -4°C (Williams et al., 2006). Unlike oak, hickory only became important in the study area after ca. 8 ka (green lines, Fig. 3). Its history parallels the slower long-term increase in temperatures during winter compared to summer. As oak pollen and summer temperatures declined in the late Holocene, hickory pollen retained its earlier abundance suggesting stable winter temperatures.

The increase in hickory in the south after 8 ka, but not in the north, marks a widening latitudinal vegetative difference. The winter temperature reconstructions generated from the full pollen assemblages show a persistent C-N difference of ~2°C (thin blue line, Fig. 3d), but a widening S-C difference from near-zero to >4°C (thin red line, Fig. 3d). An exception to this pattern developed from 4.8-3.8 ka when hickory abundance increased in the central region as oak-hickory assemblages expanded into central highland sites. As with oak, the hickory increase followed the regional decline in hemlock by 700 years on average (Fig. 3b) and did not develop in the north where the reconstructed winter temperatures declined (Fig. 3c). The winter reconstructions indicate a 2°C increase in the C-N gradient and a ~1°C decline in the S-C gradient (Fig. 3d).

### 3.3 Changing latitude of steepest gradients

The difference in the steepness of the two summer temperature gradients (C-N minus S-C, Fig. 2f) indicates:

- a southward shift in the steepest part of the gradient before 6 ka as southern areas warmed, but northern areas cooled;
- a northward shift from 4.8-3.8 ka when the northern (C-N) gradient was steeper than the southern (S-C) gradient by up to 0.8°C, similar to the cool, late-Holocene pattern since 1.8 ka (see Fig. S1 for a geographic representation of the temperature gradient); and
- a nearly uniform regional gradient (a near zero difference, Fig. 2f) between these two periods from 3.8-1.8 ka.

In winter, because the northern (C-N) gradient remained near 2°C and the southern (S-C) gradient increased from 0°C to >4°C, the steepest gradient was initially in the north, but shifted to the south by the late-Holocene. The northward oscillation in the position of the steepest segment interupted the trend from 4.8-3.8 ka when C-N was steeper than S-C by up to 1.6°C (Fig. 3f).

## 4 Discussion

### 4.1 Interpreting the long-term changes

At the time of European colonization of the northeast U.S., the LTG determined a sharp contrast between northern mixed forests and oak-hickory forests to the south (Cogbill et al., 2002). The reconstructed shifts in the LTG, therefore, provide a plausible climatic explanation for latitudinal differences in the regional vegetation history. A weak north-south gradient in summer before ca. 8.2 ka (Fig. 2e) helps to explain the early peak in oak abundance at northern sites (green lines, Fig. 2c); the polar front was likely furthest north at the time and similar summer temperatures across the region enabled oak to spread widely. When the summer LTG then steepened (Fig. 2e), oak readily declined in the north where sites began cooling (Fig. 2c) while also expanding in the south (Fig. 2a). Tree population increases south of a non-advancing range limit are not uncommon (Lloyd, 2005), and should be expected if the LTG steepened in place of uniform temperature increases or declines regionwide. Birch followed the opposite pattern as oak until the mid-Holocene, widening the vegetation difference (Fig. 2a-c) as the LTG steepened across all latitiudes.

Different directions of insolation forcing explain a northern steepening of the LTG in summer (Fig. 2f), but a southern steepening in winter (Fig. 3f). Early-to-mid Holocene insolation anomalies acted to weaken the summer LTG by preferentially heating northern continental areas, especially compared to coastal areas in the southeast. The reverse took place in winter because low winter insolation cooled low latitudes more than high latitudes, which receive little winter insolation even today (Berger, 1978). A southern steepening of the summer LTG during the early-Holocene, however, represents a departure from the insolation trend (thin line, Fig. 2f). Much of the change, prior to ca. 8 ka, corresponded with the declining influence of the Laurentide ice sheet on atmospheric waves over the Atlantic. The summer anomaly may indicate a thermodynamic response to the ice albedo anomaly (Morrill et al., 2018) rather than the year-round effect of the ice as a mechanical barrier to the flow of the jet stream (COHMAP, 1988).

Paradoxically, the presence of the ice sheet thus combined with insolation anomalies to facilitate the northward expansion of oak at 10-8 ka.

### 4.2 The mid-Holocene anomaly

The most significant departure from the insolation and ice sheet effects arose when a steep front developed in the north from 4.8-3.8 ka (Fig. 2e-f, 3e-f). The front cooled the north but limited cold outbreaks to the south. It favored northern birch populations (Fig. 2c), even as it enabled oak-hickory forests to expand into newly warmed central highlands (Fig. 4a). The changes began as temperatures fell in the north after 6.2 ka (blue lines, Fig. 2d, 3d) and were amplified when central temperatures reached their maximum at 4.8-3.8 ka (black lines, Fig. 2d, 3d). The millennial scale of this central temperature maximum has analogies at the other latitudes, such as the cluster of northern sites that warmed from 3.4-1.8 ka (Fig. 2c, 3c). They indicate that more than one fluctuation in the LTG took place with a steep front returning to the north after 1.8 ka (Fig. 2c-f).

The engimatic absence of hemlock undoubtly affected forest dynamics after 5.5 ka, but the similarity of the decline across latitudes (Fig. 3b-c) contrasts with the north-south vegetation differences 700 yrs later (Fig. 2b-c). Extensive droughts may have been important (Booth et al., 2012; Haas and McAndrews 1999; Newby et al., 2014). They caused fluctuations in hemlock abundance at some sites (Marsicek et al., 2013) and are faithfully reconstructed from fossil pollen using our methods and data (Shuman et al., 2019). Other forest influences, such as wildfire and insect outbreaks, are not widely evident (Clark et al., 1996; Oswald et al., 2016; 2020), but local ecological interactions must have shaped landscape-scale changes (e.g., potentially explaining synchroneity of the decline with drought onset at one site but not another amid localized hemlock variability; Booth et al., 2012). Regardless, hemlock's demise did not drive all of the major forest changes. Abrupt changes in coastal oak and beech populations where hemlock is rare appear consistent with local cooling (Fig. 4b; Foster et al., 2006). In the north, the simultaneous switch from hemlock to birch, another cold-tolerant tree (Fig. 2c), raises a key question: why did oak replace hemlock and other cold-adapted trees like birch and beech in the central region (Fig. 2b, 4a) – but not along the coast (Fig. 4b) or in the north as it did in the early-Holocene (Fig. 2c)?

The reconstructed LTG changes point to a plausible answer. Different trees systematically replaced hemlock by latitude because temperatures changed in opposite directions in a manner analogous to the NAO (Fig. 1c-e). Cooling forced the northern limit of abundant hemlock southward as central warming extended southern forests with little hemlock northward. Droughts amplified the pattern. Positive NAO phases similarly steepen the northern LTG today (Fig. 1e), which is consistent with isotopic evidence of a steep northern front at 4.8-3.8 ka (Fig. 4c; Kirby et al., 2002). The NAO pattern extends warming from the mid-Atlantic region into the central study area despite little change in the southern study area (Fig. 1d). Ocean cooling simultaneously develops from Labrador to Massachusetts (Fig. S2), which would explain why a narrow coastal zone of oak-beech changes (Fig. 4b) differs from the rest of the southern region (Fig. 2a).

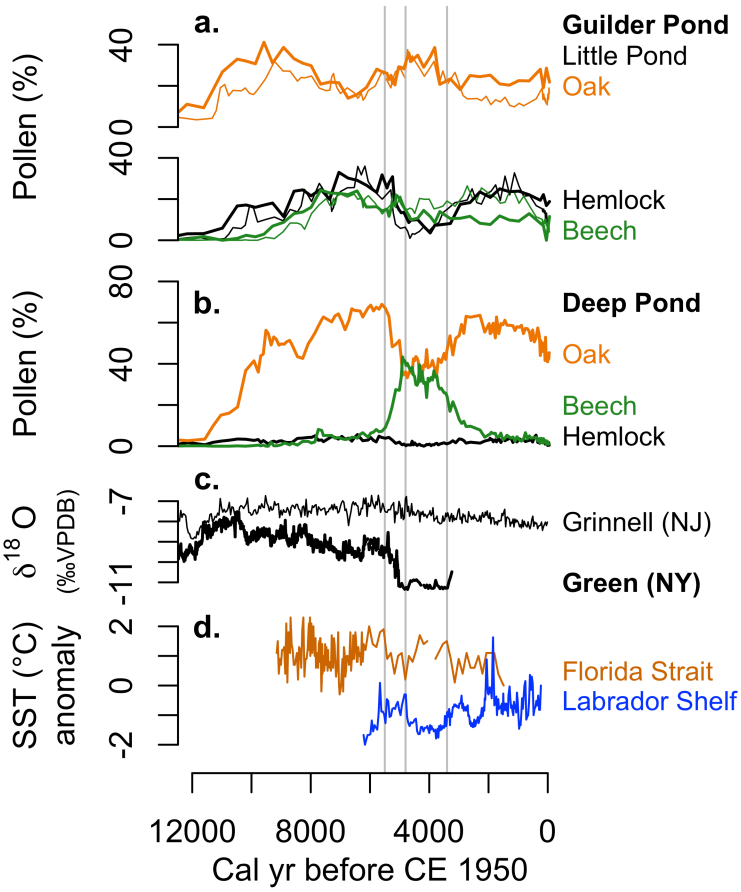


**Figure 4. Representative oak, hemlock, and beech pollen records (a) from the central region (Guilder Pond and Little Pond, Royalston; Oswald et al., 2018) are compared with b) pollen data from Deep Pond in coastal Massachusetts (Foster et al., 2006), c) lake oxygen isotope records from the southern and northern regions (Grinnell Lake, New Jersey, Zhao et al., 2010; Fayetteville Green Lake, New York, Kirby et al., 2002), and d) sea-surface temperature (SST) reconstructions from the Florida Strait (Lochte et al., 2020) and Labrador Shelf (Schmidt et al., 2012).**

A contrast between low sea-surface temperatures (SSTs) from 4.5-3.5 ka on the Labrador Shelf (Lochte et al., 2020) and high SSTs in the Florida Strait from 4.7-3.3 ka (Schmidt et al., 2012)(Fig. 4d) agrees with the patterns associated with a strong Atlantic pressure gradient today (Fig. S2). However, a NAO reconstruction from Greenland indicates a negative phase at the same time (Olsen et al., 2012), which raises questions about whether the circulation changes involved have direct analogs to the NAO at monthly to annual scales. Regardless of the relationship, the mid-Holocene oscillation coincides with millennial anomalies in North Atlantic deep water flow, wind speeds, and atmospheric circulation (Giraudeau et al., 2010; Jackson et al., 2005; O'Brien et al., 1995). Evidence of unusual climates at the same time extends from paleosol development in Nebraska's Sand Hills (Miao et al., 2007) to isotopic anomalies in Africa (Thompson et al., 2002). The patterns may relate to intrinsic atmospheric variability, particularly if ocean-atmosphere or sea-ice interactions sustained the changes (Orme et al., 2021;

Rigor et al., 2002; Thornalley et al., 2009). Alternatively, volcanic and solar variability may have been influential factors (Fletcher et al., 2013; Kobashi et al., 2017), but no clear linear correlation with external forcing is evident, potentially as expected (Renssen et al., 2006).

## 5 Conclusions

The Holocene temperature history of eastern North America includes changes in the steepness of the north-south temperature gradient, which generally responded in different directions to summer and winter insolation anomalies. Well-described Holocene forcing, however, does not explain an apparent millennial-scale latitudinal shift in the slope and position of the temperature front, which expanded oak-hickory forests into mid-latitudes as birch increased to the north from 4.8-3.8 ka. Understanding the NAO-like change may help explain the hemlock decline, associated droughts, and other mid-Holocene abrupt change events and dynamics.

## Acknowledgments

This work was supported by NSF funding to BNS (DEB-1856047) and to the Harvard Forest Long-Term Ecological Research Program (LTER-1832210). We thank two anonymous reviewers for insightful comments.

## Open Research

The analyses here depend upon fossil pollen data, which can be retrived from the Neotoma Paleoecology Database using the site names listed in Table S1 in the 'neotoma' package version 1.7.4 in R 4.0.0 (Goring et al., 2019; R Core Development Team, 2022). Chronologies were updated in R using the 'bchron' package version 4.7.4 (Parnell et al., 2008) and temperature reconstructions were generated using the 'rioja' package version 0.9-21 (Juggins, 2019). The reconstructions and median ages are available as a supplement to this manuscript and will be submitted to the NOAA NCEI Paleoclimate archive upon acceptance for publication.

## References

Barnosky, A. D., Barnosky, C. W., Nickmann, R. J., Ashworth, A. C., Schwert, D. P., & Lantz, S. W. (1988). Late Quaternary Paleoecology at the Newton Site, Bradford Co., Northeastern Pennsylvania: Mammuthus Columbi, Palynology, and Fossil Insects. *Bulletin of the Buffalo Society of Natural Sciences*, *33*, 173–184.

Berger, A. (1978). Long-term variations of caloric insolation resulting from the earth's orbital elements. *Quaternary Research*, *9*(2), 139–167.

Booth, R. K., Brewer, S., Blaauw, M., Minckley, T. A., & Jackson, S. T. (2012). Decomposing the mid-Holocene *Tsuga* decline in eastern North America. *Ecology*, *93*(8), 1841–1852. https://doi.org/10.1890/11-2062.1

Bryson, R. A. (1966). Air masses, streamlines, and the boreal forest. *Geological Society of America Bulletin*, *8*, 228.

Clark, J. S., Royall, P. D., & Chumbley, C. (1996). The Role of Fire During Climate Change in an Eastern Deciduous Forest at Devil's Bathtub, New York. *Ecology*, *77*(7), 2148–2166.

377 Cogbill, C. V., Burk, J., & Motzkin, G. (2002). The forests of presettlement New England, USA: spatial and
378 compositional patterns based on town proprietor surveys. *Journal of Biogeography*, *29*(10–11), 1279–1304.
379 https://doi.org/10.1046/j.1365-2699.2002.00757.x
380 COHMAP Members (1988). Climate changes of the last 18,000 years: observations and model simulations. *Science*,
381 *241*, 1043–1052.
382 Crucifix, M., de Vernal, A., Franzke, C., & von Gunten, L. (2017). Centennial to Millennial Climate Variability,
383 131–166. https://doi.org/10.22498/pages.25.3
384 Davis, B. A., & Brewer, S. (2009). Orbital forcing and role of the latitudinal insolation/temperature gradient.
385 *Climate Dynamics*, *32*(2–3), 143–165. http://dx.doi.org/10.1007/s00382-008-0480-9
386 Davis, M. B. (1969). Climatic changes in southern Connecticut recorded by pollen deposition at Rogers Lake.
387 *Ecology*, *50*, 409–422.
388 Davis, M. B. (1981). Outbreaks of forest pathogens in Quaternary history. *Proceedings of the Fourth International*
389 *Palynological Conference*, *3*, 216–227.
390 Deevey, E. S. (1939). Studies on Connecticut lake sediments. I. A Postglacial Climatic Chronology for Southern
391 New England. *American Journal of Science*, *237*, 691–724.
392 Dunwiddie, P. W. (1990). Postglacial vegetation history of coastal islands in southeastern New England. *National*
393 *Geographic Research*, *6*, 178–195.
394 Fastovich, D., Russell, J. M., Jackson, S. T., Krause, T. R., Marcott, S. A., & Williams, J. W. (2020). Spatial
395 Fingerprint of Younger Dryas Cooling and Warming in Eastern North America. *Geophysical Research*
396 *Letters*, *47*(22), e2020GL090031. https://doi.org/10.1029/2020GL090031
397 Fletcher, W. J., Debret, M., & Goñi, M. F. S. (2013). Mid-Holocene emergence of a low-frequency millennial
398 oscillation in western Mediterranean climate: Implications for past dynamics of the North Atlantic
399 atmospheric westerlies. *The Holocene*, *23*(2), 153–166. https://doi.org/10.1177/0959683612460783
400 Folland, C. K., Knight, J., Linderholm, H. W., Fereday, D., Ineson, S., & Hurrell, J. W. (2009). The Summer North
401 Atlantic Oscillation: Past, Present, and Future. *Journal of Climate*, *22*(5), 1082–1103.
402 https://doi.org/10.1175/2008JCLI2459.1
403 Foster, D. R., Oswald, W. W., Faison, E. K., Doughty, E. D., & Hansen, B. C. S. (2006). A climatic driver for abrupt
404 mid-Holocene vegetation dynamics and the hemlock decline in New England. *Ecology*, *87*(12), 2959–2966.

405 Giraudeau, J., Grelaud, M., Solignac, S., Andrews, J. T., Moros, M., & Jansen, E. (2010). Millennial-scale
406 variability in Atlantic water advection to the Nordic Seas derived from Holocene coccolith concentration
407 records. *Quaternary Science Reviews*, *29*(9), 1276–1287. https://doi.org/10.1016/j.quascirev.2010.02.014
408 Goring, S. J., Simpson, G. L., Marsicek, J. P., Ram, K., & Sosalla, L. (2019). neotoma: Programmatic R interface to
409 the Neotoma Paleoecological Database. R, rOpenSci. Retrieved from https://github.com/ropensci/neotoma
410 Gaudreau, D. C. (1986). *Late-Quaternary vegetational history of the Northeast: palaeological implications of*
411 *topographic patterns in pollen data* (PhD Thesis). Yale University, New Haven.
412 Hurrell, J. W., Kushnir, Y., Ottersen, G., & Visbeck, M. (2003). *The North Atlantic Oscillation*. *Geophys. Monogr.*
413 *Ser.* (Vol. 134). https://doi.org/10.1029/134GM01
414 Ibe, R. A. (1982). *Quaternary palynology of five lacustrine deposits in the Catskill Mountain region of New York*
415 (PhD Thesis). New York University.
416 Jackson, M. G., Oskarsson, N., Trønnes, R. G., McManus, J. F., Oppo, D. W., Grönvold, K., et al. (2005). Holocene
417 loess deposition in Iceland: Evidence for millennial-scale atmosphere-ocean coupling in the North Atlantic.
418 *Geology*, *33*(6), 509–512. https://doi.org/10.1130/G21489.1
419 Juggins, S. (2019). rioja: Analysis of Quaternary Science Data (Version 0.9-21). Retrieved from https://CRAN.R-
420 project.org/package=rioja
421 Kalnay, E., Kanamitsu, M., Kistler, R., Collins, W., Deaven, D., Gandin, L., et al. (1996). The NCEP/NCAR 40-
422 Year Reanalysis Project. *Bulletin of the American Meteorological Society*, *77*(3), 437–472.
423 https://doi.org/10.1175/1520-0477(1996)077<0437:TNYRP>2.0.CO;2
424 Kirby, M. E., Mullins, H. T., Patterson, W. P., & Burnett, A. W. (2002). Late glacial-Holocene atmospheric
425 circulation and precipitation in the northeast United States inferred from modern calibrated stable oxygen
426 and carbon isotopes. *Geological Society of America Bulletin*, *114*(10), 1326–1340.
427 https://doi.org/10.1130/0016-7606(2002)114<1326:lghaca>2.0.co;2
428 Kobashi, T., Menviel, L., Jeltsch-Thömmes, A., Vinther, B. M., Box, J. E., Muscheler, R., et al. (2017). Volcanic
429 influence on centennial to millennial Holocene Greenland temperature change. *Scientific Reports*, *7*(1),
430 1441. https://doi.org/10.1038/s41598-017-01451-7
431 Larsen, D. J., Miller, G. H., Geirsdóttir, Á., & Ólafsdóttir, S. (2012). Non-linear Holocene climate evolution in the
432 North Atlantic: a high-resolution, multi-proxy record of glacier activity and environmental change from

433 Hvítárvatn, central Iceland. *Quaternary Science Reviews*, *39*, 14–25.
434 https://doi.org/10.1016/j.quascirev.2012.02.006
435 Levesque, A. J., Cwynar, L. C., & Walker, I. R. (1997). Exceptionally steep north-south gradients in lake
436 temperatures during the last deglaciation. *Nature*, *385*(6615), 423–426.
437 Lloyd, A. H. (2005). Ecological histories from Alaskan tree lines provide insight into future change. *Ecology*, *86*(7),
438 1687–1695.
439 Lochte, A. A., Schneider, R., Kienast, M., Repschläger, J., Blanz, T., Garbe-Schönberg, D., & Andersen, N. (2020).
440 Surface and subsurface Labrador Shelf water mass conditions during the last 6000 years. *Climate of the*
441 *Past*, *16*(4), 1127–1143. https://doi.org/10.5194/cp-16-1127-2020
442 Maenza-Gmelch, T. E. (1997a). Holocene vegetation, climate, and fire history of the Hudson Highlands,
443 southeastern New York, USA. *The Holocene*, *7*, 25–37.
444 Maenza-Gmelch, T. E. (1997b). Vegetation, climate, and fire during the late-glacial-Holocene transition at Spruce
445 Pond, Hudon Highlands, southeastern New York, USA. *Journal of Quaternary Science*, *12*, 15–24.
446 Marsicek, J. P., Shuman, B., Brewer, S., Foster, D. R., & Oswald, W. W. (2013). Moisture and temperature changes
447 associated with the mid-Holocene Tsuga decline in the northeastern United States. *Quaternary Science*
448 *Reviews*, *80*(3), 333–342. https://doi.org/10.1016/j.quascirev.2013.09.001
449 Miao, X., Mason, J. A., Johnson, W. C., & Wang, H. (2007). High-resolution proxy record of Holocene climate
450 from a loess section in Southwestern Nebraska, USA. *Palaeogeography, Palaeoclimatology,*
451 *Palaeoecology*, *245*(3–4), 368–381. https://doi.org/10.1016/j.palaeo.2006.09.004
452 Morrill, C., Lowry, D. P., & Hoell, A. (2018). Thermodynamic and Dynamic Causes of Pluvial Conditions During
453 the Last Glacial Maximum in Western North America. *Geophysical Research Letters*, *45*(1), 335–345.
454 https://doi.org/10.1002/2017GL075807
455 O'Brien, S. R., Mayewski, P., Meeker, L. D., Twickler, M. S., & Whitlow, S. I. (1995). Complexity of Holocene
456 climate as reconstructed from a Greenland ice core. *Science*, *270*, 1962.
457 Olsen, J., Anderson, N. J., & Knudsen, M. F. (2012). Variability of the North Atlantic Oscillation over the past
458 5,200 years. *Nature Geoscience*, *5*(11), 808–812. https://doi.org/10.1038/ngeo1589

Orme, L. C., Miettinen, A., Seidenkrantz, M.-S., Tuominen, K., Pearce, C., Divine, D. V., et al. (2021). Mid to late-Holocene sea-surface temperature variability off north-eastern Newfoundland and its linkage to the North Atlantic Oscillation. *The Holocene*, *31*(1), 3–15. https://doi.org/10.1177/0959683620961488

Oswald, W. W., Doughty, E. D., Foster, D. R., Shuman, B. N., & Wagner, D. L. (2016). Evaluating the role of insects in the middle-Holocene Tsuga decline. *The Journal of the Torrey Botanical Society*, *144*(1), 35–39. https://doi.org/10.3159/TORREY-D-15-00074.1

Oswald, W. W., Foster, D. R., Shuman, B. N., Chilton, E. S., Doucette, D. L., & Duranleau, D. L. (2020). Conservation implications of limited Native American impacts in pre-contact New England. *Nature Sustainability*, *3*(3), 241–246. https://doi.org/10.1038/s41893-019-0466-0

Oswald, W. W., Foster, D. R., Shuman, B. N., Doughty, E. D., Faison, E. K., Hall, B. R., et al. (2018). Subregional variability in the response of New England vegetation to postglacial climate change. *Journal of Biogeography*, *45*(10), 2375–2388. https://doi.org/10.1111/jbi.13407

Overpeck, J. T. (1985). A pollen study of a late Quaternary peat bog, south-central Adirondack Mountains, New York. *Geological Society of America Bulletin*, *96*, 145–154.

Overpeck, J. T., Webb III, T., & Prentice, I. C. (1985). Quantitative interpretation of fossil pollen spectra: dissimilarity coefficients and the method of modern analogs. *Quaternary Research*, *23*, 87–108.

Paciorek, C. J., Goring, S. J., Thurman, A. L., Cogbill, C. V., Williams, J. W., Mladenoff, D. J., et al. (2016). Statistically-estimated tree composition for the northeastern United States at Euro-American settlement. *PloS One*, *11*(2), e0150087.

Paciorek, C. J., Cogbill, C. V., Peters, J. A., Williams, J. W., Mladenoff, D. J., Dawson, A., & McLachlan, J. S. (2021). The forests of the midwestern United States at Euro-American settlement: Spatial and physical structure based on contemporaneous survey data. *PLOS ONE*, *16*(2), e0246473. https://doi.org/10.1371/journal.pone.0246473

Parnell, A. C., Haslett, J., Allen, J. R. M., Buck, C. E., & Huntley, B. (2008). A flexible approach to assessing synchroneity of past events using Bayesian reconstructions of sedimentation history. *Quaternary Science Reviews*, *27*(19â€“20), 1872–1885. https://doi.org/10.1016/j.quascirev.2008.07.009

Pielke, R. A., & Vidale, P. L. (1995). The boreal forest and the polar front. *Journal of Geophysical Research: Atmospheres*, *100*(D12), 25755–25758. https://doi.org/10.1029/95JD02418

Prentice, I. C., Bartlein, P. J., & Webb III, T. (1991). Vegetation and climate changes in eastern North America since the last glacial maximum: A response to continuous climatic forcing. *Ecology*, *72*, 2038–2056.

R Core Development Team. (2022). *R: A language and environment for statistical computing.* R Foundation for Statistical Computing, Vienna, Austria. Retrieved from http://www.R-project.org

Reimer, P. J., Austin, W. E. N., Bard, E., Bayliss, A., Blackwell, P. G., Ramsey, C. B., et al. (2020). The IntCal20 Northern Hemisphere Radiocarbon Age Calibration Curve (0–55 cal kBP). *Radiocarbon*, *62*(4), 725–757. https://doi.org/10.1017/RDC.2020.41

Renssen, H., Goosse, H., & Muscheler, R. (2006). Coupled climate model simulation of Holocene cooling events: oceanic feedback amplifies solar forcing. *Climate of the Past*, *2*, 79–90.

Rigor, I. G., Wallace, J. M., & Colony, R. L. (2002). Response of Sea Ice to the Arctic Oscillation. *Journal of Climate*, *15*(18), 2648–2663. https://doi.org/10.1175/1520-0442(2002)015<2648:ROSITT>2.0.CO;2

Routson, C. C., McKay, N. P., Kaufman, D. S., Erb, M. P., Goosse, H., Shuman, B. N., et al. (2019). Mid-latitude net precipitation decreased with Arctic warming during the Holocene. *Nature*, *568*(7750), 83–87. https://doi.org/10.1038/s41586-019-1060-3

Schmidt, M. W., Weinlein, W. A., Marcantonio, F., & Lynch-Stieglitz, J. (2012). Solar forcing of Florida Straits surface salinity during the early Holocene. *Paleoceanography*, *27*(3). https://doi.org/10.1029/2012PA002284

Seager, R., Battisti, D. S., Yin, J., Gordon, N., Naik, N., Clement, A. C., & Cane, M. A. (2002). Is the Gulf Stream responsible for Europe's mild winters? *Quarterly Journal of the Royal Meteorological Society*, *128*(586), 2563–2586. https://doi.org/10.1256/qj.01.128

Shuman, B. N., Bartlein, P., Logar, N., Newby, P., & Webb, T. (2002). Parallel climate and vegetation responses to the early-Holocene collapse of the Laurentide Ice Sheet. *Quaternary Science Reviews*, *21*, 1793–1805.

Shuman, B. N., Marsicek, J., Oswald, W. W., & Foster, D. R. (2019). Predictable hydrological and ecological responses to Holocene North Atlantic variability. *Proceedings of the National Academy of Sciences*, *116*(13), 5985–5990. https://doi.org/10.1073/pnas.1814307116

Spear, R. W., Davis, M. B., & Shane, L. C. K. (1994). Late Quaternary History of Low- and Mid-Elevation Vegetation in the White Mountains of New Hampshire. *Ecological Monographs*, *64*(1), 85–109.

514 Spear, R.W. (1981). *The history of high-elevation vegetation in the White Mountains of New Hampshire* (PhD
515 Thesis). University of Minnesota.
516 Suter, S. M. (1985). Late-glacial and Holocene vegetational history in southeastern Massachusetts: a 14,000 year
517 pollen record. *Current Research in the Pleistocene*, *2*, 87–89.
518 Thompson, J. R., Carpenter, D. N., Cogbill, C. V., & Foster, D. R. (2013). Four Centuries of Change in Northeastern
519 United States Forests. *PLOS ONE*, *8*(9), e72540. https://doi.org/10.1371/journal.pone.0072540
520 Thompson, L. G., Mosley-Thompson, E., Davis, M. E., Henderson, K. A., Brecher, H. H., Zagorodnov, V. S., et al.
521 (2002). Kilimanjaro Ice Core Records: Evidence of Holocene Climate Change in Tropical Africa. *Science*,
522 *298*(5593), 589–593. https://doi.org/10.1126/science.1073198
523 Thornalley, D. J. R., Elderfield, H., & McCave, I. N. (2009). Holocene oscillations in temperature and salinity of the
524 surface subpolar North Atlantic. *Nature*, *457*(7230), 711–714.
525 Toney, J. L., Rodbell, D. T., & Miller, N. G. (2003). Sedimentologic and palynologic records of the last deglaciation
526 and Holocene from Ballston Lake, New York. *Quaternary Research*, *60*(2), 189–199.
527 https://doi.org/10.1016/S0033-5894(03)00093-0
528 Vannière, B., Power, M. J., Roberts, N., Tinner, W., Carrión, J., Magny, M., et al. (2011). Circum-Mediterranean
529 fire activity and climate changes during the mid-Holocene environmental transition (8500-2500 cal. BP).
530 *The Holocene*, *21*(1), 53–73. http://dx.doi.org.libproxy.uwyo.edu/10.1177/0959683610384164
531 Watts, W. A. (1979). Late Quaternary vegetation of central Appalachia and the New Jersey coastal plain. *Ecological*
532 *Monographs*, *49*, 427–469.
533 Whitehead, D. R., & Crisman, T. (1978). Paleolimnological studies of small New England (U.S.A.) ponds. I: Late
534 glacial and postglacial trophic oscillations. *Polskie Archiwum Hydrobiologii*, *25*, 471–481.
535 Whitehead, D. R., & Jackson, S. T. (1990). The Regional Vegetational History of the High Peaks (Adirondack
536 Mountains) New YORK. *New York State Museum Bulletin*, *478*, III–27.
537 Whitmore, J., Gajewski, K., Sawada, M., Williams, J., Shuman, B., Bartlein, P. J., et al. (2005). An updated modern
538 pollen-climate-vegetation dataset for North America. *Quaternary Science Reviews*, *24*, 1828–1848.
539 Willard, D. A., Bernhardt, C. E., Korejwo, D. A., & Meyers, S. R. (2005). Impact of millennial-scale Holocene
540 climate variability on eastern North American terrestrial ecosystems: pollen-based climatic reconstruction.
541 *Global and Planetary Change*, *47*(1), 17–35. https://doi.org/10.1016/j.gloplacha.2004.11.017

542 Williams, J. W., Shuman, B. N., Bartlein, P. J., Whitmore, J., Gajewski, K., Sawada, M., et al. (2006). An Atlas of
543 Pollen-Vegetation-Climate Relationships for the United States and Canada. *American Association of*
544 *Stratigraphic Palynologists Foundation, Dallas, TX*.
545 Williams, J. W., Grimm, E. C., Blois, J. L., Charles, D. F., Davis, E. B., Goring, S. J., et al. (2018). The Neotoma
546 Paleoecology Database, a multiproxy, international, community-curated data resource. *Quaternary*
547 *Research*, *89*(1), 156–177. https://doi.org/10.1017/qua.2017.105
548 Woodward, F. I. (1987). *Climate and Plant Distribution*. (R. S. K. Barnes, H. J. B. Birks, E. F. Connor, J. L. Harper,
549 & R. T. Paine, Eds.). Cambridge: Cambridge University Press.
550 Vose, R.S., Applequist, S., Durre, I., Menne, M.J., Williams, C.N., Fenimore, C., et al. (2014). Improved Historical
551 Temperature and Precipitation Time Series For U.S. Climate Divisions. *Journal of Applied Meteorology*
552 *and Climatology*. http://dx.doi.org/10.1175/JAMC-D-13-0248.1
553 Zhao, Y., Yu, Z. C., & Zhao, C. (2010). Hemlock (Tsuga canadensis) declines at 9800 and 5300 cal yr BP caused by
554 Holocene climatic shifts in northeastern North America. *The Holocene*, *20*, 877–886.
555 https://doi.org/10.1177/0959683610365932
556
557
558
559

*Geophysical Research Letters*

Supporting Information for

# A Millennial-Scale Oscillation in Latitudinal Temperature Gradients along the Western North Atlantic during the Mid-Holocene

Bryan N. Shuman[1], Ioana C. Stefanescu[1], Laurie D. Grigg[2], David R. Foster[3], and W. Wyatt Oswald[4]

[1] Department of Geology and Geophysics, University of Wyoming, Laramie, WY.

[2] Department of Earth and Environmental Sciences, Norwich University, Northfield, VT.

[3] Harvard Forest, Petersham, MA.

[4] Marlboro Institute for Liberal Arts and Interdisciplinary Studies, Emerson College, Boston, MA.

## Contents of this file



## Additional Supporting Information (Files uploaded separately)



## Introduction

The supporting information includes figures showing the reconstructed temperatures versus latitude for key time intervals (Fig. S1) and modern sea-surface temperature anomalies associated with changes in the position of the steepest portion of the latitudinal temperature gradient, LTG (Fig. S2). Additional data tables include a list of fossil pollen records used in the analysis (Table S1) as well as the summer and winter temperature reconstructions for each site (Date Sets S1-S2) and for each latitudinal cluster of sites (Date Sets S3-S4). Data Sets S3 and S4 also include the reconstructed gradients between latitudinal clusters shown in Figures 2 and 3.

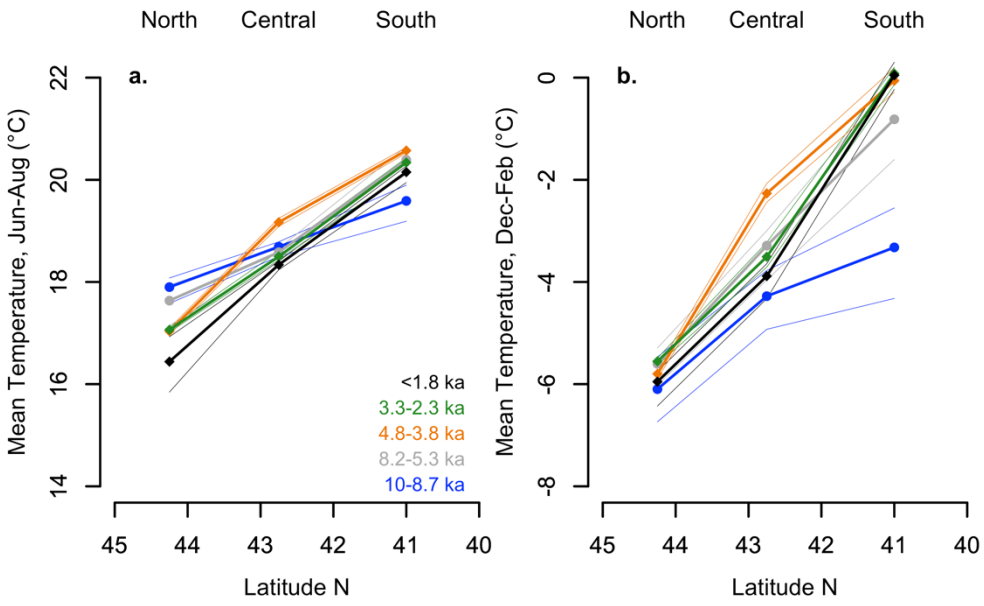


**Figure S1.** Reconstructed latitudinal temperature gradients for a) summer (July-August) and b) winter (December-February) are plotted for 10-8.2 ka (dark blue), 8.2-5.3 ka (gray), 4.8-3.8 ka (orange), 3.3-2.3 ka (green) and since 1.8 ka (black). Mean temperatures from each latitude (Fig. 2d, 3d) are plotted as the median (bold) and 95% range (thin lines) of the seasonal mean temperature for each time interval. 500-yr intervals between periods are excluded to differentiate the patterns regardless of age control uncertainties.

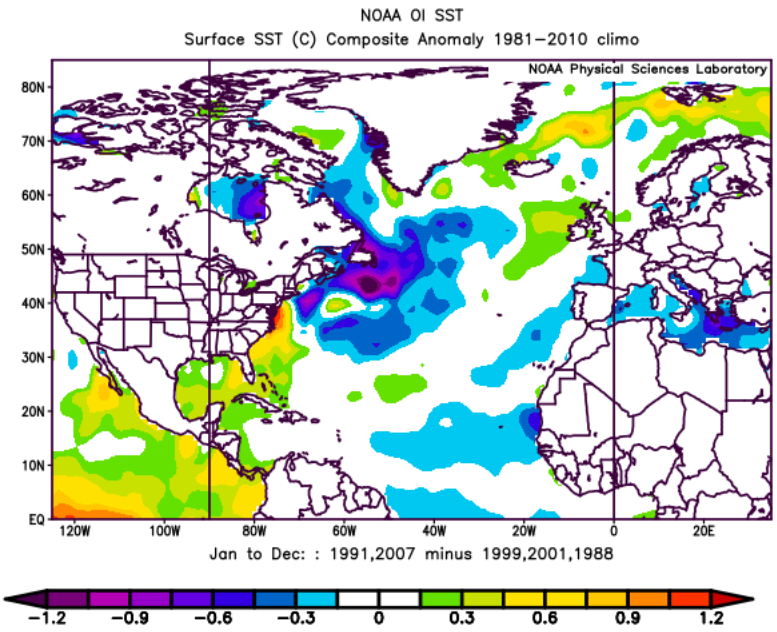


**Figure S2.** Map of mean sea-surface temperature (SST) composite anomalies shows the expected change from a steep southern LTG to a steep northern LTG (such as developed at 4.8 ka). Data derive from the NOAA Optimum Interpolation (OI) SST dataset (maps generated at https://psl.noaa.gov/cgi-bin/data/composites/) for the years since 1981 when the latitudinal temperature gradient in the study region was steepest north of 42.75°N (1991, 2007) minus those when it was steepest south of 42.75°N (1988, 1999, 2001). The SST anomalies represent years with a strong (Figure 1c) minus weak (Figure 1b) Atlantic pressure gradient.

The modern changes in the LTG, used to identify the years for the composite anomaly maps here and in Fig. 1 were calculated using annual temperatures from climate division data (Vose et al., 2014) to calculate temperature differences between latitudinal zones. Climate Division temperature data from Vermont (statewide mean), western Massachusetts (division 1), and Connecticut (statewide mean) represent the northern, central, and southern regions respectively. Composite anomaly maps showing changes in surface pressure (Fig. 1b,c) were generated using the NCEP/NCAR Reanalysis (Kalnay et al., 1996) for the five years when the steepest gradient was furthest north or south based on the C-N (MA-VT) minus S-C (CT-MA) difference. Maps were generated using tools from the NOAA/ESRL Physical Sciences Laboratory, Boulder, Colorado at https://psl.noaa.gov/.

**Table S1.** Fossil pollen records

| Site | Latitude | Longitude | Elevation | Median Sample Frequency (yr/sample) | Citation |
|---|---|---|---|---|---|
| Ballston Lake | 42.9498 | -73.8533 | 82 | 156 | Toney et al., 2003 |
| Balsam Lake | 42.0288 | -74.6042 | 880 | 107 | Ibe R.A., 1982 |
| Berry Pond, East | 42.6201 | -71.0868 | 43 | 269 | Oswald et al., 2018 |
| Berry Pond, West | 42.5051 | -73.3167 | 610 | 46 | Whitehead and Crisman, 1978 |
| Black Pond | 41.3279 | -70.7927 | 13 | 91.5 | Oswald et al., 2018 |
| Blood Pond | 42.0802 | -71.9611 | 227 | 90.5 | Oswald et al., 2018 |
| Brandreth Bog | 43.9167 | -74.6833 | 582 | 202 | Overpeck, J.T. 1985 |
| Deep Pond, Falmouth | 41.5640 | -70.6357 | 27 | 69 | Oswald et al., 2018 |
| Deep Pond, Taunton | 41.8822 | -71.0120 | 8 | 365 | Oswald et al., 2018 |
| Deer Lake Bog | 44.0333 | -71.8333 | 1213 | 496.5 | Spear, R.W. 1981 |
| Eagle Lake Bog | 44.1667 | -71.6667 | 955 | 414 | Spear, R.W. 1981 |
| Green Pond | 42.5671 | -72.5108 | 97 | 483 | Oswald et al., 2018 |
| Guilder Pond | 42.1086 | -73.4372 | 622 | 303.5 | Oswald et al., 2018 |
| Heart Lake | 44.1824 | -73.9696 | 686 | 373 | Whitehead and Jackson. 1990 |
| Kinsman Pond | 44.1333 | -71.7333 | 1162 | 565.5 | Spear, R.W. 1981 |
| Knob Hill Pond | 44.3604 | -72.3730 | 378 | 74 | Oswald et al., 2018 |
| Little Pond, Royalston | 42.6760 | -72.1929 | 308 | 143 | Oswald et al., 2018 |
| Little Willey Pond | 43.2917 | -71.1781 | 259 | 156.5 | Oswald et al., 2018 |
| Lost Pond | 44.2469 | -71.2514 | 656 | 425 | Spear et al., 1994 |
| Mohawk Pond | 41.8112 | -73.2927 | 381 | 326.5 | Guadreau, D.C. 1986 |
| No Bottom Pond | 41.2833 | -70.2083 | 0 | 314 | Dunwiddie, P.W. 1990 |
| North Pond | 42.6517 | -73.0534 | 593 | 204 | Whitehead and Crisman. 1978 |
| Rogers Lake | 41.3525 | -72.2992 | 16 | 173 | Davis, M.B. 1969 |
| Spring Lake | 41.6739 | -76.3500 | 364 | 352 | Barnowsky et al., 1988 |
| Spruce Pond | 41.2369 | -74.1833 | 208 | 72.5 | Maenza-Gmelch, 1997a |
| Sutherland Pond | 41.3914 | -74.0378 | 392 | 88 | Maenza-Gmelch, 1997b |
| Tannersville Bog | 41.0389 | -75.2639 | 282 | 120.5 | Watts, W.A. 1979 |
| Twin Ponds | 44.0614 | -72.5787 | 409 | 213 | Grigg et al., in review |
| Umpawaug Pond | 41.3060 | -73.4495 | 149 | 109 | Oswald et al., 2018 |
| Uncle Seth's Pond | 41.4331 | -70.6646 | 20 | 233.5 | Oswald et al., 2018 |
| Upper Wallface Pond | 44.1483 | -74.0557 | 981 | 761.5 | Whitehead and Jackson. 1990 |
| Ware Pond | 42.4825 | -70.8823 | 9 | 215 | Oswald et al., 2018 |
| West Side Pond | 41.8545 | -73.2566 | 407 | 224 | Oswald et al., 2018 |
| Winneconnet Pond | 41.9667 | -71.1167 | 22 | 227.5 | Suter, S.M. 1985 |